Journal of Statistical Physics, Vol. 62, Nos. 3/4, 1991

Diffusion and Propagation in Triangular Lorentz Lattice Gas Cellular Automata

X. P. Kong[1] and E. G. D. Cohen[1]

Received August 17, 1990

The diffusion process of point particles moving on regular triangular and random lattices, randomly occupied with stationary scatterers (a Lorentz lattice gas cellular automaton), is studied, for strictly deterministic scattering rules, as a function of the concentration of the scatterers. In addition to the normal and various kinds of retarded diffusion found before on the regular square lattice, straight-line propagation through the scatterers is observed.

KEY WORDS: Normal and retarded diffusion; propagation; lattice gas; cellular automata; triangular lattice; deterministic scattering rules.

1. INTRODUCTION

In a number of previous papers[1-4] we have investigated diffusion in Lorentz lattice gas cellular automata (CA)[5] on a square lattice. There point particles move, all with the same speed, along the bonds of a regular square lattice, the sites of which are randomly occupied by stationary scatterers. Depending on the scattering rule, four different types of diffusive behavior of the particles through the scatterers were observed, leading to four classes of diffusion[4]: (1) normal diffusion, where the distribution function (d.f.) of the point particle is Gaussian and therefore the mean square displacement $\Delta(t) \sim t$ (class I); (2) anomalous diffusion, where the d.f. is non-Gaussian, but $\Delta(t) \sim t$, so that still a diffusion coefficient can be defined (class II); (3) abnormal diffusion, where the d.f. is non-Gaussian and $\Delta(t) \sim t^{1-\alpha}$, with $0 < \alpha < 1$ (class III); (4) no diffusion, where the particles are all trapped in closed orbits and $\Delta(t)$ remains finite (class IV). While the first class obtained for all probabilistic scattering rules considered, the other three pertained to deterministic scattering rules. We always restricted ourselves to deterministic scattering rules in the presence

[1] The Rockefeller University, New York, New York 10021.

0022-4715/91/0200-0737$06.50/0

of two kinds of scatterers: scatterers that upon collision scattered the moving particle either to the left or to the right. It appeared that introducing a slight—but still deterministic—modification of the deterministic scattering rules in the fixed scatterer models, viz., by allowing the scatterers to change from one kind to the other upon a collision with a moving particle, thus introducing a flipping scatterer model,[1] reduced the diffusion process from the unusual behavior of classes II–IV to the normal behavior of class I. By changing the relative concentration of scatterers in a mixed model[6] with probabilistic and deterministic scattering rules, dynamical phase transitions could be obtained between lattice gas CA that behave according to the classes I–IV.[4]

This experimentally discovered new and rich behavior of diffusion has not yet been treated theoretically in any adquate way. Only models with purely probabilistic scattering rules, where the diffusion is normal and the only problem is the calculation of the diffusion coefficient for a given (probabilistic) scattering rule as a function of the concentration of the scatterers, have been treated extensively with existing methods of kinetic theory by Ernst, Binder, and Van Velzen.[7–9] There the deviations from the Boltzmann approximation can be calculated in a more or less standard manner by using cluster expansions and related techniques of kinetic theory. It is interesting to note that the application of these kinetic methods by Van Velzen[9] to the mirror model,[1] though intended to apply to fixed scatterers, produced results in accordance with flipping scatterers. Due to the presence of closed (periodic) orbits, implying infinitely long memory effects, it seems likely that new methods will be necessary to understand the general behavior of deterministic models from a microscopic point of view. To the best of our knowledge, no such methods are available at present either in kinetic theory or in the mathematical literature, where it appears that so far only probabilistic models have been considered. For that reason it seemed prudent to try to isolate features of a general nature of the deterministic models as much as possible. Since we had investigated the dependence of the diffusion process on the nature of the scattering rules always on a regular square lattice, it seemed natural to do likewise on a random lattice, thus introducing a new type of randomness in the problem. Since the way we constructed this random lattice led to a triangulation of the plane, we also studied, for comparison, the diffusion on a regular triangular lattice. The results of these new investigations are reported in this paper and can be summarized as follows.

1. The randomness or regularity of the lattice does not in general change the basic nature (i.e., the class) of the diffusion process for a given scattering rule for the fixed scatterers.

2. While on the regular square lattice the motion of the particles through the scatterers was always a diffusion process, on the regular triangular lattice with flipping scatterers, straight-line propagation (in a coarse-grained sense) of the particle through the scatterers was discovered. In this case the mean square displacement is $\Delta(t) \sim t^2$ and undamped propagation along lattice directions occurs. This behavior obtained for flipping scatterers on a fully occupied lattice only.

The organization of this paper is as follows. In Section 2, we introduce the two models by specifying the collision rules. Basic quantities for describing diffusion processes are defined, the Boltzmann approximation to the diffusion coefficient is given, and the simulation method is described. Section 3 is concerned with our results for a regular triangular lattice fully occupied with fixed scatterers. Anomalous diffusion and a connection with the percolation problem are discussed for the fixed scatterer models. Section 4 shows that for both models on a regular triangular lattice fully occupied with flipping scatterers, the motion of the particle through the lattice is by pure propagation. In Section 5, results for a partially occupied regular triangular lattice are presented, where both normal and abnormal diffusion are found. Section 6 discusses the diffusion on a random triangular lattice. Finally, in Section 7 we give a summary and discussion.

2. THE MODELS, THE BOLTZMANN APPROXIMATION, AND THE SIMULATION METHOD

2.1. The Models

We consider a two-dimensional triangular lattice with lattice sites randomly occupied with stationary scatterers, such that there is at most one scatterer at each lattice site. The concentration C of the scatterers is the ratio of the total number of scatterers N to the number of lattice sites M, so that $0 < C = N/M \leqslant 1$. In addition, point particles are randomly put on the lattice, which have the same speed and velocity directions restricted to be along the bonds of the lattice, so that the particles always stay on the lattice. The particles travel one lattice distance per unit time in the direction of their velocities. It is convenient to set the speed of the particles as well as the lattice distance both equal to one. When a moving particle meets a stationary scatterer at an occupied lattice site, its velocity direction will change according to a prescribed deterministic scattering (or collision) rule; the rules we considered will be discussed below. The six possible velocity directions that can occur at a lattice site are shown in Fig. 1a and will be denoted by $i = 1,..., 6$. Five different models will be considered,

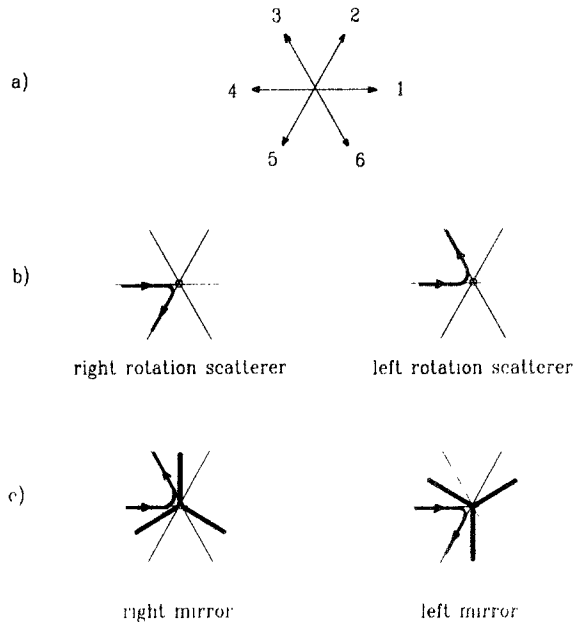

Fig. 1. (a) Velocity directions on the triangular lattice; (b) rotation scatterers of model 1; (c) mirror scatterers of model 2, where the heavy lines represent a (tree star) mirror and the designation of right and left is arbitrary. The arrowed trajectories indicate typical reflection paths. For clarity here as well as in the other figures the particle trajectories have been curved at collisions.

corresponding to five different collision rules. We remark that there are no collision between the point particles themselves.

2.1.1. Model 1. In the first model the scatterers simply rotate the velocity of the colliding particle over $\pm 2\pi/3$ (widest angle it can turn)[2] clockwise or counterclockwise, depending on whether one has right-hand scatterers (R) or left-hand scatterers (L) (cf. Fig. 1b). If the scatterers do not change their character during a collision, i.e., each always remains a right or a left scatterer, the model is called a fixed scatterer model (or model 1A); if, on the other hand, they do change upon collision with a point particle from right to left scatterers (or vice versa), the model is called a flipping scatterer model (or model 1B). Model 1A is a generalization to the triangular lattice of a model introduced by Gunn and Ortuño.[10]

2.1.2. Model 2. In the second model the scatterers behave like double-sided mirrors and reflect the oncoming particle as if it was a photon

[2] We remark that, for the fully occupied lattice, if the moving particle turns $\pm\pi/3$ upon colliding with a scatterer, the model is equivalent to the same model on a honeycomb lattice.

hitting a mirror (cf. Fig. 1c). While on a square lattice there is an obvious way to occupy the lattice sites with mirrors to achieve this (viz., along the bonds of the two sublattices, at angles $\pi/4$ or $3\pi/4$, respectively, with those of the basic lattice), on a triangular lattice a two-sided "tree star mirror" system has to be in place at each occupied lattice site, as illustrated in Fig. 1c. There are two possible positions of these tree star mirrors, which we will call right (R) and left (L) mirrors, respectively. Again, if the mirrors have fixed positions, the model is called a fixed mirror model (or model 2A) and if the mirrors change, upon collision, from one kind (R, L) to the other (L, R), the model is called a flipping mirror model (or model 2B). Model 2 is a generalization to a triangular lattice of the model introduced by Ruijgrok and Cohen on a square lattice.[1]

We remark that for $C=1$, i.e., for a lattice fully occupied with scatterers, the particle trajectories of model 1 and model 2 map into each other. Furthermore, model 1B and model 2A are time-reversal invariant, while the others are not. We also note that while for the fixed models (1A and 2A) there is no interaction between the particles, in the flipping models (1B and 2B) the flipping of the mirrors by the colliding particles introduces interactions between particles and mirrors, so that, in particular, the particles do not move independently of each other anymore. Only when one considers a single moving particle in the flipping models does this interparticle interaction disappear. Thus, one can distinguish here the case of one or more than one moving particle. In the following we will restrict ourselves to the case of one moving particle.

The macroscopic process that we study in these models is the diffusion of the moving particle(s) through the scatterers as a function of the nature and concentration of the scatterers. If the mean square displacement $\Delta(t) \equiv \langle x^2(t) \rangle$ of a particle in a particular direction, the x axis say,[3] is proportional to the time t for long times, a diffusion coefficient D can be defined by

$$D = \lim_{t \to \infty} D(t) = \lim_{t \to \infty} \frac{\langle x^2(t) \rangle}{2t} \tag{1}$$

where the brackets $\langle \cdot \rangle$ indicate an average over initial configurations of the particles and the scatterers. For a normal diffusion process, the probability distribution function $P(\mathbf{r}, t)$ to find a particle at the lattice site $\mathbf{r}$ at time t, when it was at the origin at $t=0$, is Gaussian. Then, not only are its second moments with respect to x, y, and z equal to $\Delta(t)$ and $\sim t$, but all its odd moments vanish and its even moments can be expressed in

[3] Since we only consider isotropic systems, all directions are equivalent.

terms of $\Delta(t)$, so that all its cumulants vanish. In particular, the kurtosis $K(t)$, defined by

$$K \equiv \frac{\langle x^4 \rangle - 3\langle x^2 \rangle^2}{\langle x^2 \rangle^2} \tag{2}$$

vanishes.

In this paper we will restrict ourselves exclusively to the case of equal concentrations of right and left scatterers, i.e., $C_R = C_L = C/2$.

2.2. The Boltzmann Approximation

The Boltzmann approximation for the diffusion process assumes that a moving particle never collides twice with the same scatterer, so that no memory effects occur. Introducing then the one-particle distribution function $f_i(\mathbf{r}, t)$, which is proportional to the probability to find a particle with velocity direction i at the lattice site $\mathbf{r}$ at time t, the Boltzmann approximation leads to a discrete Boltzmann equation for $f_i(\mathbf{r}, t)$ on the lattice of the form[2]

$$f_i(\mathbf{r} + \mathbf{e}_i, t+1) = \sum_{j=1}^{6} T_{ij} f_j(\mathbf{r}, t), \qquad i = 1, \ldots, 6 \tag{3}$$

where $\mathbf{e}_i$ is the unit vector in the velocity direction i. The 6×6 collision matrix $\mathbf{T}$ in (3) is given by

$$\mathbf{T} = \begin{pmatrix} -C & 0 & C/2 & 0 & C/2 & 0 \\ 0 & -C & 0 & C/2 & 0 & C/2 \\ C/2 & 0 & -C & 0 & C/2 & 0 \\ 0 & C/2 & 0 & -C & 0 & C/2 \\ C/2 & 0 & C/2 & 0 & -C & 0 \\ 0 & C/2 & 0 & C/2 & 0 & -C \end{pmatrix} \tag{4}$$

where the entries correspond to the 6×6 possible directions of pre- and postcollision velocities on a triangular lattice.

The Boltzmann approximation D_B to the diffusion coefficient D is easily obtained[2] from Eqs. (3) and (4) and reads

$$D_B = \frac{1}{2C} - \frac{1}{4} \tag{5}$$

where the term $-1/4$ is the usual "ballistic" contribution to the diffusion coefficient due to the discreteness of the lattice.[2,5]

2.3. Computer Simulations

In our computer simulations we use a unit cell of 1024×1024 lattice sites for the regular lattice and 50×50 lattice sites for the random lattice and periodic boundary conditions[4] for the configurations of the randomly placed scatterers. About 2600 particles for the regular lattice and 1000 particles for the random lattice are randomly placed on the latice. We let them move on the "infinite checkerboard," in order to be able to compute $\Delta(t)$, etc. The calculations were executed up to $t = 2^{14}$ time steps.

The results are obtained in two steps. First an average is made over all particles for one simulation run; then further averages are computed over the results of many runs to obtain the final results with their statistical errors. The number of runs used is determined by the smoothness of the results. For the regular lattice, ten runs is usually enough; however, many more runs are needed for the random lattice because of the limited number of particles in each run. The standard deviations of the mean are plotted as the error bars of the data points in the figures. When no error bars are visible, they are inside the symbols.

In order to determine the precise nature of the diffusion process, we sometimes have to determine the behavior of the probability distribution function $P(\mathbf{r}, t)$. Since we are dealing with isotropic systems, the radial distribution function

$$\hat{P}(r, t) \equiv \int_0^{2\pi} \int_r^{r+1} d\theta \, dr \, P(\mathbf{r}, t)$$

is generated, where r and θ are the polar coordinates of $\mathbf{r}$. This is done by counting the number of particles between r and $r+1$ at time t, when they started from the origin at $t = 0$. For comparison

$$\hat{P}_G(r, t) \equiv \int_0^{2\pi} \int_r^{r+1} d\theta \, dr \, P_G(\mathbf{r}, t)$$

of the Gaussian distribution function $P_G(\mathbf{r}, t)$, determined by the measured diffusion coefficient, is usually drawn with $\hat{P}(r, t)$.

3. DIFFUSION ON A FULLY OCCUPIED LATTICE (FIXED SCATTERERS)

3.1. Diffusion

In this section we present our results for model A for the case that every lattice site is occupied by a fixed scatterer, so that $C = 1$ and

[4] Details for the random lattice can be found in ref. 20.

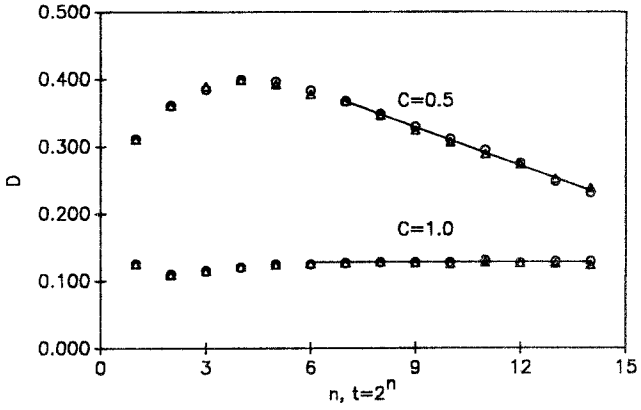

Fig. 2. Time dependence of the diffusion coefficient D for $C=1$ and $C=0.5$ of model 1A (open circles) and model 2A (open triangles). The drawn line for the $C=0.5$ case indicates ($\sim -\log t$) behavior.

$C_R = C_L = 1/2$. We shall see that the diffusive behavior at this concentration is rather different from that at all other concentrations, but similar to that on a square lattice for all $C_L = C_R$.

In Fig. 2 we show the time dependence of the diffusion coefficient $D(t)$, as defined by Eq. (1), for the fixed scatterer models 1A and 2A. We see that after a short time, $D(t)$ reaches a constant value. In spite of the fact that then $\Delta(t) \sim t$, the kurtosis $K(t)$ does not vanish and, in fact, shows a behavior $\sim \log t$ (cf. Fig. 3). This implies anomalous (class II) diffusion

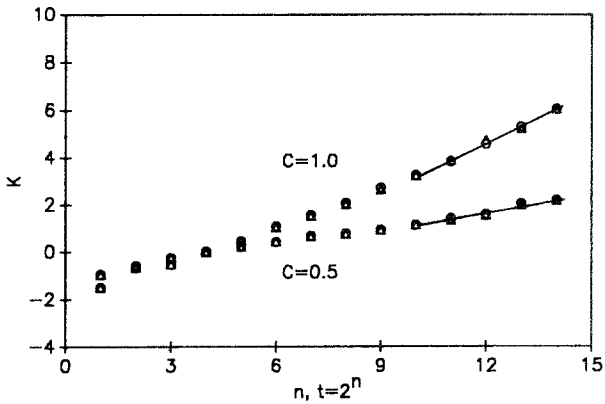

Fig. 3. Time dependence of the kurtosis K for fixed scatterers and $C=1$ and $C=0.5$. Symbols used here are the same as in Fig. 2.

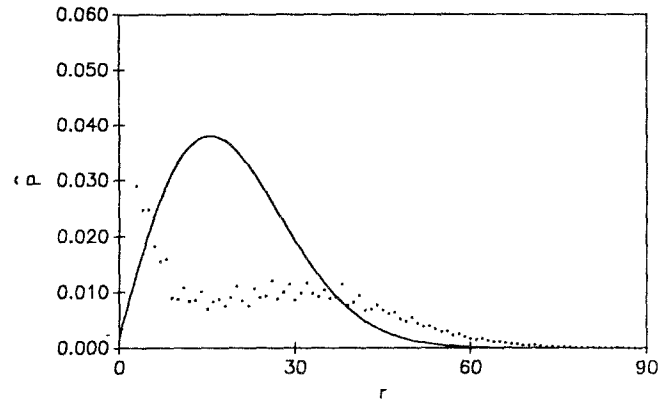

Fig. 4. Radial density distribution function $\hat{P}(r, t)$ as a function of distance r for fixed scatterers and $C = 1$ at $t = 1000$; the drawn curve is a Gaussian $\hat{P}_G(r, t)$ with the measured D. For $r = 0$, $\hat{P} = 0.12$.

and a non-Gaussian distribution function $P(\mathbf{r}, t)$, as is ilustrated in Fig. 4. The large peak at the origin is due to closed orbits, where the particle trajectories exhibit a periodic motion.

3.2. Trajectories As Hulls of Percolation Clusters

In this subsection, we want to demonstrate that the trajectories of the moving particle for the $C = 1$, fixed scatterer models (model 1A and model 2A) are so-called hull generating walks (HGW),[11] viz., they trace out the boundaries (hulls) of the percolation clusters, at the percolation threshold, of the site percolation problem of the triangular lattice. In the site percolation problem, each site has a probability p to be occupied, and the occupied sites form clusters if they are neighbors. The size of the cluster—number of occupied sites in the cluster—can vary from cluster to cluster, but the average size is an increasing function of p. The percolation threshold, $p = 1/2$ for the site percolation on a triangular lattice,[12] is where clusters with an infinite size start to form. In the $C = 1$ case of our fixed models, occupancy of a site by one particular kind of scatterer, say a left scatterer, is chosen as the occupancy of that site in the percolation sense. Then a right scatterer at the same site means that this site is not occupied. Since we have $C_L = C_R = 1/2$, each site has a probability $p = 1/2$ to be occupied, so that the lattice is at the percolation threshold. Figure 5 shows for model 2A (mirrors) that the trajectories trace out the boundaries between clusters of occupied sites and unoccupied sites (model 2A illustrates this more clearly than model 1A).[5]

[5] We remark that, like the fixed models on the square lattice,[2] the trajectory of the moving particle can be considered as a smart kinetic walk (SKW)[14] on a triangular lattice.

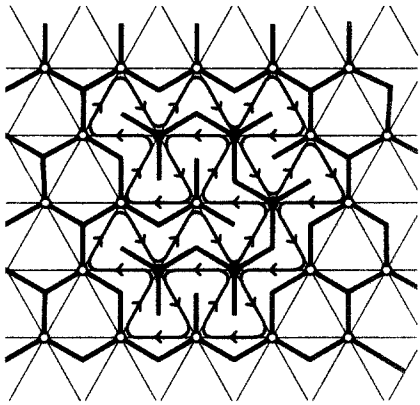

Fig. 5. A typical particle trajectory, for fixed scatterers and $C = 1$ (illustrated for model 2A), as the boundary between two percolation clusters. The black (white) dots indicate occupied (unoccupied) lattice sites.

It has been argued[13] that these hulls themselves have scaling behavior and that at the threshold, their distribution function n_s - number of hulls with size s per bond—has the form[13]

$$n_s \sim s^{-\tau} \tag{6}$$

where s is the size of the hull, i.e., the trajectory length of the moving particle, and τ is the scaling exponent. Furthermore, the hulls are fractals, and the mean square end-to-end distance $\langle R_h^2 \rangle$ on these fractals is related to the fractal dimension d_f by the scaling relation[13]

$$\langle R_h^2 \rangle \sim s^{2/d_f} \tag{7}$$

Figure 6 shows a typical fractal generated by a moving particle at time $t = 2^{16}$.

The above scaling relations allow a deeper understanding of why the means square displacement $\Delta(t)$ of the particles is proportional to t, although no normal diffusion takes place. This can be achieved by connecting these scaling relations to a dynamical property of our diffusion process, viz. the mean square displacement $\Delta(t)$. For, $\Delta(t)$ at time t can be written as a sum of contributions of closed trajectories (on hulls with sizes smaller than t) and of open trajectories (on hulls with sizes larger than t):

$$\Delta(t) = \langle R^2(t) \rangle = \sum_{s=0}^{t} s^{1-\tau} s^{2/d_f} + \sum_{s=t}^{\infty} s^{1-\tau} t^{2/d_f} \tag{8}$$

where $s^{1-\tau} = s \cdot n_s$ is the probability of having a hull with size s. Replacing the sums by integrals yields

$$\Delta(t) \sim t^{2-\tau+2/d_f} \tag{9}$$

Using then the hyperscaling relation $\tau - 1 = 2/d_f$,[13] we see that indeed $\Delta(t) \sim t$, in agreement with our measurements. This then also is consistent with the scaling laws (6) and (7).

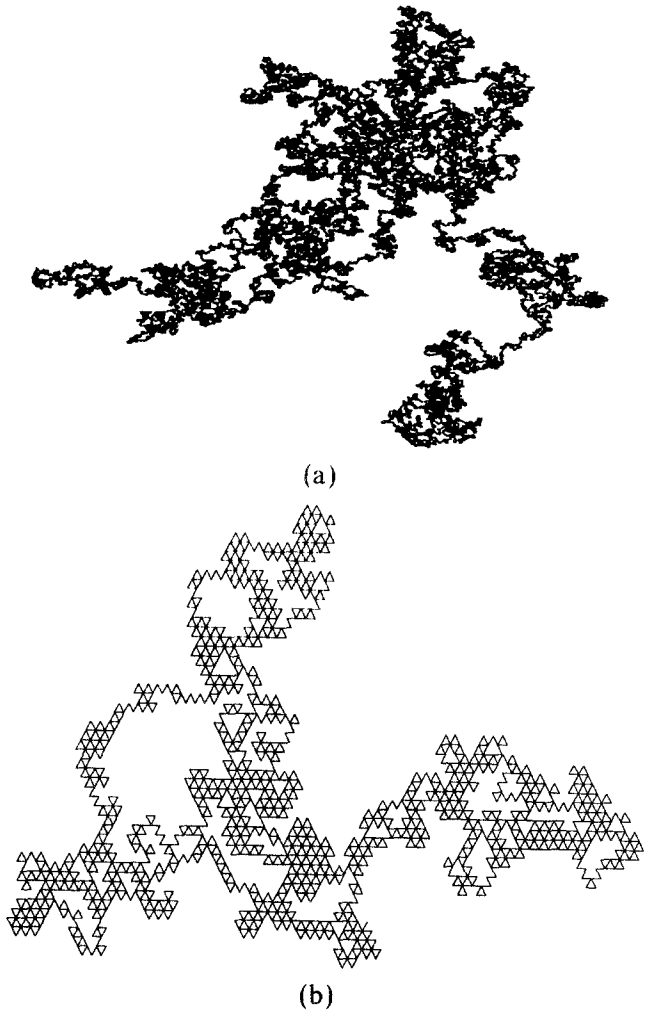

Fig. 6. (a) A typical fractal generated by a moving particle through fixed scatterers and $C = 1$ at $t = 2^{16}$; (b) a blowup of part of (a), where the underlying lattice structure can be seen.

4. PROPAGATION ON A FULLY OCCUPIED LATTICE (FLIPPING SCATTERERS)

A very remarkable behavior is obtained on a regular triangular lattice with flipping scatterers (model 1B and model 2B) when the lattice is fully occupied by scatterers ($C=1$). One can convince onself that if one starts a particle at $t=0$ at an initial position with an initial velocity along a particular lattice direction, it will propagate through the lattice in three possible directions. These directions depend on the states (R or L) of at most four neighboring scatterers at $t=0$: there is a probability of 3/8 to propagate in a direction that makes an angle of $\pm\pi/3$ with the initial particle velocity and a probability of 1/4 to propagate in the opposite direction of the initial particle velocity. A typical example is sketched in Fig. 7, while in Fig. 8 the detailed scattering mechanism is shown that leads to the propagation. One sees that a moving particle, arriving at any lattice site A, can either be scattered "forward" (Fig. 8a) and move to point B, such that it travels a (projected) distance of 1/2 in its (coarse-grained) propagation direction, or be scattered "backward" (Fig. 8b) to point C and travel the same distance. In the latter case, it will take six additional time steps (via points C D E C D) to arrive again at the site A (now with flipped mirror) and then move "forward" to point B. Thus the average forward speed of the moving particle $\bar{v}_p$ is given by

$$\bar{v}_p = \frac{1}{2}\frac{1}{\frac{1}{2}+7\cdot\frac{1}{2}} = \frac{1}{8} \tag{10}$$

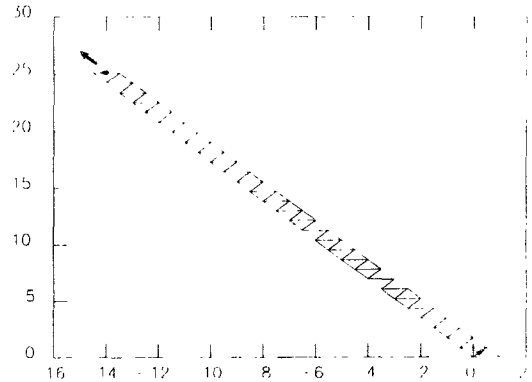

Fig. 7. A typical propagation for flipping scatterers and $C=1$ at $t=200$. The first ($t=0$) and the last ($t=200$) steps have been marked with arrows, while the propagation direction is indicated by a heavy arrow. The x (y) axis indicates the x (y) coordinate of the particle. One sees that the propagation proceeds alternatively forward and backward, such that the average speed of propagation is 1/8.

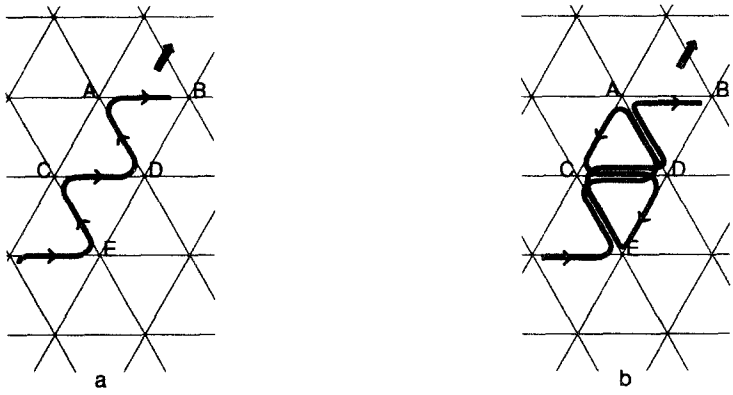

Fig. 8. Detailed propagation mechanism. Both possibilities of scattering at point A (R or L) end up at point B and lead to a (coarse-grained) propagation along the direction indicated by a heavy arrow. (a) Forward scattering directly from A to B; (b) backward scattering from A to C, which leads via C D E C D again to forward scattering from A to B. For clarity the particle trajectories have been curved and displaced from the lattice bonds.

This is confirmed by the data shown in Fig. 9, where we also see that this propagation speed is quickly reached.

The propagation implies that in this case the mean square displacement $\Delta(t) \sim t^2$. This should be distinguished from the enhanced diffusion discussed in the literature in connection with Lévy flights and Lévy walks,[15] where the same behavior of $\Delta(t)$ is found, but where still difussion, albeit faster than normal, in all directions in the plane takes place, while here propagation in one particular direction only occurs.

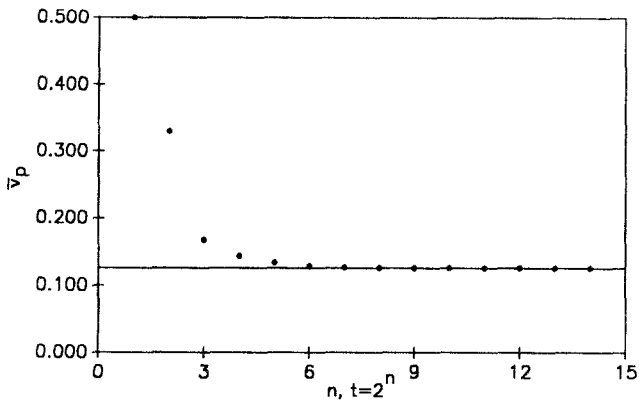

Fig. 9. Time dependence of the average speed $\bar{v}_p$ of propagation; the straight line is the $\bar{v}_p = 1/8$ line.

We remark that this propagating behavior depends on the chosen scattering rule. If one were to choose a scattering rule of rotation over $\pi/3$ at collision, the resulting motion would be normal diffusion on a honeycomb lattice.

5. DIFFUSION ON A PARTIALLY OCCUPIED LATTICE

5.1. Fixed Scatterers (Model 1A and Model 2A)

Unlike the anomalous diffusion (class II) on the square lattice for $C<1$ ($C_L = C_R$), the diffusion on the triangular lattice becomes abnormal (class III) for $C<1$ ($C_L = C_R$) for both models. Indeed, Fig. 2 shows that the diffusion coefficient $D(t)$, as defined by (1), decreases with t and appears to approach zero for large t. When a straight line is drawn through the points for the longest times in Fig. 2, a time dependence $D(t) \sim -\log t$ is found. This abnormal diffusion is therefore even slower than that found in the mixed lattice gas model on the square lattice[4,6] as well as in the continuous Ehrenfest wind-tree model,[16-18] which exhibited a power law behavior, with $\Delta(t) \sim t^{1-\alpha}$ $(0<\alpha<1)$. Figure 3 shows that the kurtosis increases with time, approximately $\sim \log t$, indicating a localization of the distribution function near the origin because of closed orbits.

5.2. Flipping Scatterers (Model 1B and Model 2B)

Although at $C=1$ the flipping models do not exibit any diffusive behavior, since there is pure propagation, at $C<1$ these models exhibit

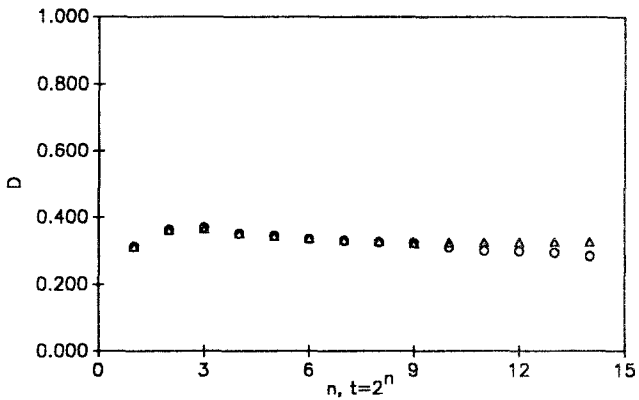

Fig. 10. Time dependence of D of model 1B (open circles) and model 2B (open triangles) for $C=0.5$.

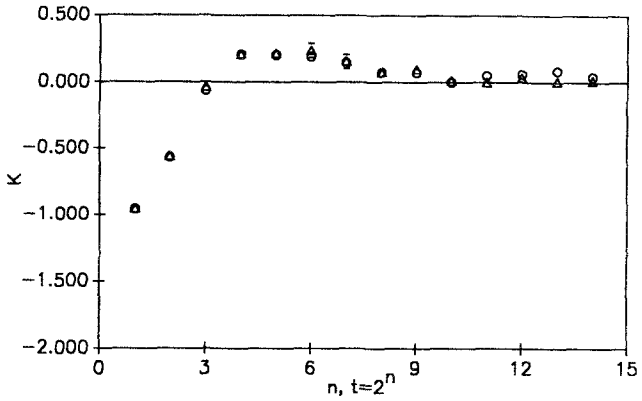

Fig. 11. Time dependence of K of model 1B (open circles) and model 2B (open triangles) for $C = 0.5$.

normal diffusion, as was also found for the flipping mirror model on the square lattice. Figure 10 shows the time dependence of the diffusion coefficients for models 1 and 2 for $C = 1/2$. One sees that for not too long times, D approaches a constant value, which appears to differ, however, for the two models. Figure 11 indicates that the kurtosis goes to zero at about the same time as the diffusion coefficient reaches a constant value. Together with the Gaussian probability density distribution implied by Fig. 12, this suggests that our data are consistent with a normal diffusion process (class I) for these intermediate densities.

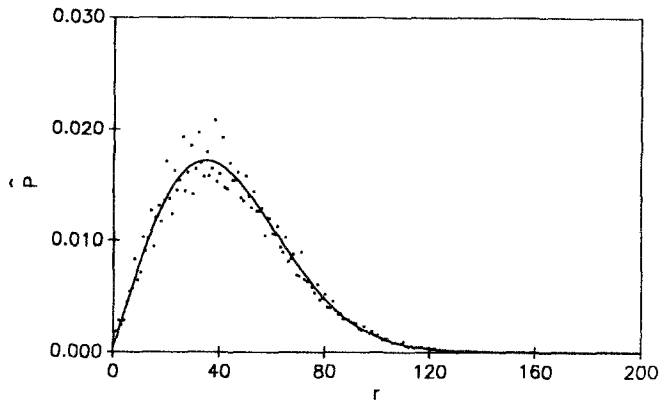

Fig. 12. Radial density distribution function $\hat{P}(r, t)$ for flipping scatterers of model 1 and model 2 and $C = 0.5$ at $t = 2048$; the drawn curve is a Gaussian with the measured D.

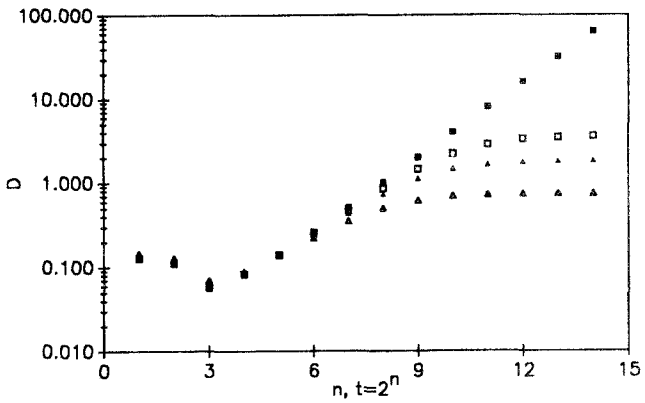

Fig. 13. Time dependence of D for flipping scatterers and several high concentrations in a $\log_{10} D(t)$ versus $\log_2 t$ plot for $C = 1$ (filled squares); $C = 0.99$ (open squares); $C = 0.98$ (filled triangles); $C = 0.90$ (open triangles).

By studying the behavior at large concentrations, where C is near 1, one sees, however, that the approach to this normal behavior becomes very slow as C approaches 1 and if fact includes an increasingly large regime where the diffusion coefficient $D(t)$ increases approximately linearly with time, leading to a diffusive behavior with $\Delta(t) \sim t^2$ (cf. Fig. 13). This diffusive $\Delta(t) \sim t^2$ behavior for $C = 1 - \varepsilon$ with $\varepsilon \ll 1$ must approach the

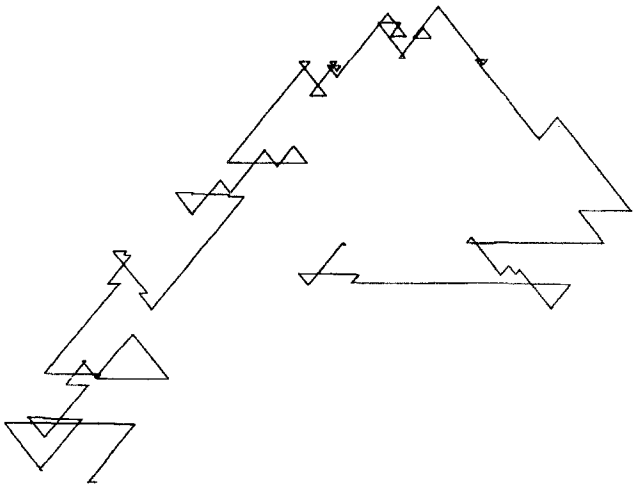

Fig. 14. A typical trajectory of the moving particle for flipping mirrors for $C = 0.99$ and $t = 2^{16}$.

propagating behavior with $\Delta(t) \sim t^2$ that obtains for $C = 1$. As far as we can tell, a direct transition of normal diffusion to propagation occurs via ever-increasing values of D, bypassing an enhanced diffusion regime, where $\Delta(t) \sim t^{1+\alpha}$, which $0 < \alpha < 1$. There seems to be no connection, therefore, with Lévy flights. We note that the initial part of $D(t)$, up to $t = 2^5$, is for all C coincident with the $D(t)$ of the $C = 1$ case (cf. Fig. 13). Furthermore, the length of this coincidence scales as $(1 - C)^{-1}$, which is proportional to the average distance between two unoccupied sites. This reflects the increasingly long time needed for the ultimate approach of $D(t)$ to a constant value, when C approaches 1 (cf. Fig. 13). This final constant value of $D(t)$ is due to the randomization of the many linear trajectory pieces (cf. Fig. 14) that occur, after a sufficiently long time. The $C = 1$ case represents, therefore, a singular case.

6. DIFFUSION ON A RANDOM TRIANGULAR LATTICE

The main purpose of studying nonregular lattices is to investigate whether significant differences will occur when the regularity of the basic lattice is destroyed and replaced, for instance, by a random lattice. In that case a new random element is introduced and the question is to what extent this will annihilate the peculiar properties of the diffusion in the deterministic scattering rule models, when compared to the normal diffusion that occurs in the probabilistic scattering rule models. The construction of a random lattice is not unique, so that the results reported below must be viewed as pertaining to a particular type of random lattice only.

Here we used the type of random lattice with periodic boundary conditions described in ref. 19. This lattice is constructed from a random distribution of points in a large square in the plane (the unit cell), with periodic boundary conditions. To determine the distribution of the bonds, sets of three points are considered; if the area contained in a circle through a given set of three points not contain any other point, then bonds are drawn between them to form a triangle. This procedure guarantees an approximate isotropy and the absence of crossed bonds and is easily implemented numerically (for details, see ref. 20). The random lattice so constructed triangulates the plane and has an average coordination number of six (cf. Fig. 15), so that the closest regular lattice to it is the regular triangular lattice. After construction of the random lattice we put scatterers on all its sites. Since, in general, no straight line passes through any lattice site, the moving particle has to make a turn at every site. We consider therefore only the case $C = 1$, equal concentration of both kinds of scatterers, and the scattering rule we implemented here is similar to the one used in model 1, i.e., upon collision, the moving particle will turn the

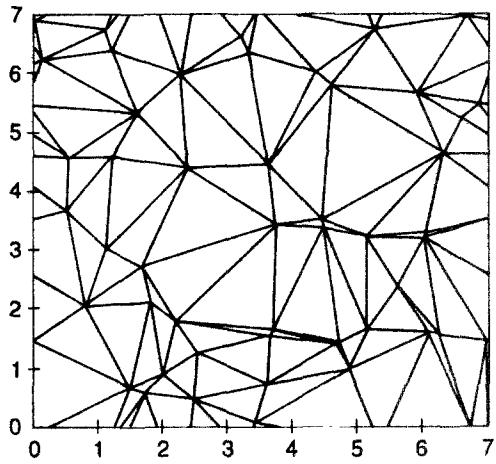

Fig. 15. An example of a random lattice with 7×7 sites.

widest angle possible to the right if colliding with a right scatterer, or to the left if colliding with a left scatterer. Although the average length of the bonds of the random lattice was equal to one, their individual lengths can be very different from one. Hence, unlike the regular lattice cases, a moving particle does not arrive at a lattice site at each time step. Because of the limitation of our computer facility, we could only generate lattices with 2500 sites, which may have caused some boundary effects in our results in the long-time regime. Since we put only 1000 particles on the lattice in each run, we needed many more runs to get statistics as good as that for the regular lattice, discussed before.

6.1. Fixed Scatterers

In this case it proved difficult to obtain clear-cut results. The time dependences of both the diffusion coefficient $D(t)$ and the kutrosis $K(t)$ were determined. Up to $t = 2^{10}$ the data (cf. (Fig. 16) are consistent with anomalous diffusion (class II), since D seems to approach a constant and K differs from zero (cf. Fig. 17). However, one cannot exclude that the puzzling behavior for the largest observed times may indicate a different long-time behavior. This long-time behavior might also be caused by the small size of the lattice, since we have unit cells of 50×50 sites only.

6.2. Flipping Scatterers

In this case the diffusion appears to be normal, in striking contrast to the propagation that occurs on the regular triangular lattice. In fact, the

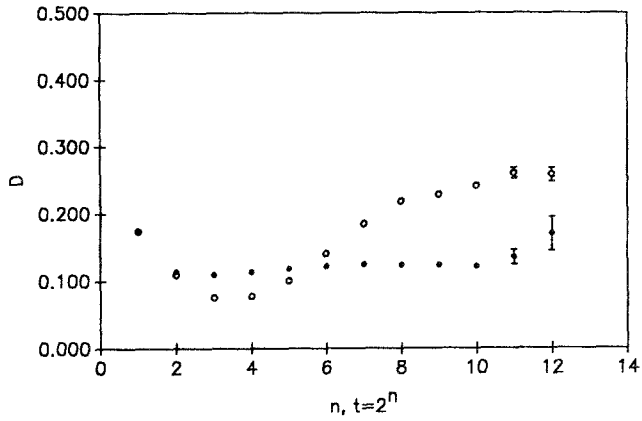

Fig. 16. Time dependence of D for fixed scatterers (filed circles) and flipping scatterers (open circles) on a random lattice.

behavior of this model appear to be like that for the flipping mirror model on a regular square latice, in that the diffusion coefficient $D(t)$ approaches a constant value D, while the kurtosis K approaches zero (cf. Figs. 16 and 17). We note that the value D for the flipping model is about twice that for the fixed model. This is due to the occurrence of regular triangular lattice-like patches in which propagation occurs.

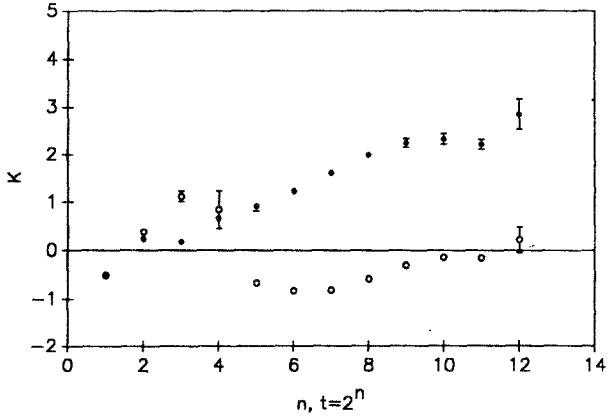

Fig. 17. Time dependence of K for fixed scatterers (filled circles) and flipping scatterers (open circles) on a random lattice.

7. SUMMARY AND DISCUSSION

1. The diffusive behavior on regular square and triangular lattices not fully occupied by equal numbers of fixed right and left scatterers is similar, in that it is non-Gaussian in both cases; there is a difference in detail, however, in that the mean square displacement is proportional to the time in the first case (class II) and grows slower than that in the second case (class III). For flipping scatterers the behavior is again similar on the two lattices in that the diffusion is normal on both lattices. There is a considerable difference, however, in their concentration dependence. For, while the coefficient $CD(C)$ varies mildly from 1/2 for $C \approx 0$ to $\approx 1/4$ for $C = 1$ for the square lattice, it increases from a value of $CD \approx 1/3$ for $C \approx 0$ to an infinite value at $C = 1$, when propagation occurs, for the triangular lattice. While in the former case, the time it takes for $D(t)$ to reach its asymptotic value is roughly independent of the concentration (always being about 2000 time steps), in the latter case this time increases indefinitely $\sim 1/(1 - C)$ when C approaches 1.

2. The diffusion on a fully occupied random (triangular-like) lattice seems to be like that on a square lattice, in that it appears to be anomalous for fixed scatterers and normal for flipping scatterers. Thus, the randomness of the lattice does not guarantee normal diffusion. The random or deterministic character of the scattering rules is therefore in this case more important in determining the nature of the diffusion process than the randomness or regularity of the underlying lattice on which the diffusion takes place.

3. The behavior found for the flipping models only obtains for strictly deterministic scattering rules. If one introduces a flipping probability α $(0 \leqslant \alpha \leqslant 1)$, so that for $\alpha = 0$ the fixed and for $\alpha = 1$ the flipping scattering models are obtained, respectively, then we find that for $0 < \alpha < 1$, always normal diffusion occurs.

Thus, it appears that the introduction of a probabilistic element in the scattering rules destroys the abnormal diffusive behavior found for strictly deterministic rules. It also destroys the unique connectivity of the deterministic trajectories, a feature it has in common with a class of reversible cellular automaton systems considered by Hasslacher and Meyer.[21] Since these authors uncovered a connection between such CA and knot theory, one could wonder whether not such a connection also exists for our deterministic scattering lattice gas CA. This might hold in particular for those models on fully occupied square or triangulair lattices, which are time reversible and represent lattice gas cellular automata at criticality.

ACKNOWLEDGMENTS

The authors would like to thank Dr. H. C. Ren for providing the program of constructing the random lattice, as well as Dr. B. Hasslacher and Dr. X. N. Wu for stimulating discussions. Part of this work was supported by Department of Energy grant no. DE-FG02-88ER13847.

REFERENCES

1. Th. W. Ruijgrok and E. G. D. Cohen, *Phys. Lett. A* **133**:4838 (1989).
2. X. P. Kong and E. G. D. Cohen, *Phys. Rev. B* **40**:4838 (1989).
3. X. P. Kong and E. G. D. Cohen, *J. Stat. Phys.* (1991).
4. X. P. Kong and E. G. D. Cohen, *Physica D* **47**:9 (1991).
5. U. Frisch, B. Hasslacher, and Y. Pomeau, *Phys. Rev. Lett.* **56**:1505 (1986).
6. P. M. Binder, *Complex Systems* 3:1 (1989).
7. M. H. Ernst and P. M. Binder, *J. Stat. Phys.* **51**:981 (1988).
8. M. H. Ernst and G. A. Van Velzen, *J. Phys. A* **22**:4611 (1989).
9. G. A. Van Velzen, Lattice Lorentz gases, Ph.D. thesis, University of Utrecht (1990).
10. J. M. F. Gunn and M. Ortuño, *J. Phys. A* **18**:L1035 (1985).
11. R. M. Ziff, *Physica D* **38**:377 (1989).
12. D. Stauffer, *Introduction to Percolation Theory* (Taylor and Francis, London, 1985).
13. R. M. Ziff, *Phys. Rev. Lett.* **56**:545 (1986).
14. A. Weinrib and S. A. Trugman, *Phys. Rev. B* **31**:2993 (1985).
15. M. F. Schlesinger, *Annu. Rev. Phys. Chem.* **39**:269 (1988); *Physica D* **38**:305 (1989).
16. P. Ehrenfest, *Collected Scientific Papers* (North-Holland, Amsterdam, 1959), p. 229.
17. E. H. Hauge and E. G. D. Cohen, *J. Math. Phys.* **10**:397 (1969).
18. W. W. Wood and F. Lado, *J. Comp. Phys.* 7:528 (1971).
19. N. H. Christ, R. Friedberg, and T. D. Lee, *Nucl. Phys. B* **202**:89 (1982).
20. R. Friedberg and H. C. Ren, *Nucl. Phys. B* **235**[FS11]:310 (1984).
21. B. Hasslacher and D. A. Meyer, Preprint (January 1990).